



HAL
open science

Characterization of rolling and longitudinal shear creeps for cross laminated timber panels

Charlotte Allemand, Arthur Lebée, Manuel Manthey, Gilles Forêt

► To cite this version:

Charlotte Allemand, Arthur Lebée, Manuel Manthey, Gilles Forêt. Characterization of rolling and longitudinal shear creeps for cross laminated timber panels. International Network on Timber Engineering Research - INTER - Meeting 53, Aug 2021, Online, France. hal-04390708

HAL Id: hal-04390708

<https://hal.science/hal-04390708>

Submitted on 16 Jan 2024

HAL is a multi-disciplinary open access archive for the deposit and dissemination of scientific research documents, whether they are published or not. The documents may come from teaching and research institutions in France or abroad, or from public or private research centers.

L'archive ouverte pluridisciplinaire **HAL**, est destinée au dépôt et à la diffusion de documents scientifiques de niveau recherche, publiés ou non, émanant des établissements d'enseignement et de recherche français ou étrangers, des laboratoires publics ou privés.

CHARACTERIZATION OF ROLLING AND LONGITUDINAL SHEAR CREEPS FOR CROSS LAMINATED TIMBER PANELS

Charlotte Allemand, Centre Scientifique et Technique du Bâtiment (CSTB), Champs-sur-Marne and Laboratoire Navier, UMR 8205, Ecole des Ponts ParisTech, Univ Gustave Eiffel, CNRS, Marne-la-vallée, France (charlotte.allemand@enpc.fr)

Arthur Lebée, Laboratoire Navier, UMR 8205, Ecole des Ponts ParisTech, Univ Gustave Eiffel, CNRS, Marne-la-vallée, France

Manuel Manthey, Centre Scientifique et Technique du Bâtiment (CSTB), Champs-sur-Marne, France

Gilles Forêt, Laboratoire Navier, UMR 8205, Ecole des Ponts ParisTech, Univ Gustave Eiffel, CNRS, Marne-la-vallée, France

Keywords: rolling-shear , creep , cross laminated timber , long-term behavior , longitudinal shear

1 Introduction

Everywhere around the world, high timber buildings are rising. The construction of these new buildings is possible thanks to the mainstreaming of some engineering products such as cross-laminated timber panels (CLT) and glued laminated timber (GLT). Those panels gained in popularity for several reasons. First, they are a more sustainable solution than concrete designs. Second, the prefabrication process makes them easy to assemble on site. CLT panels also have a high dimensional stability under variation of moisture content compared to other timber products. Because of all those advantages, high buildings up to 80-meters, such as the Mjøsa tower in Norway, are being erected. CLT panels are used both as walls and floors in those constructions.

Rolling and longitudinal shear deformations are involved in the mechanical response of those panels. Shear failure can occur for CLT panels loaded out-of-plane but also when they are under in-plane shear stresses (*Brandner et al.*, 2016). The value of the longitudinal shear modulus $G_{l,mean}^0$ for short-term lies between 440 and 880 MPa depending

on the strength class of the wood (*Eurocode-5*, 2004). In the rolling-shear direction, the short-term modulus $G_{r,mean}^0$ for short-term lies between 50 and 200 MPa (*Ehrhart and Brandner*, 2018; *Franzoni, Lebée, Lyon, et al.*, 2016; *Zhou et al.*, 2014; *Perret et al.*, 2018). Large differences between the studies are due to the difficulty to obtain a pure shear stress and to represent the behaviour of cross layers. Additionally, the sawing pattern and aspect ratio of the board are of importance for CLT (*Krabbe*, 1960; *Aicher and Dill-Langer*, 2000; *Ehrhart and Brandner*, 2018; *Perret et al.*, 2019).

Wood is a material subject to creep and this phenomenon must be investigated to correctly design timber buildings as it amplifies the short-term deflections. The first study of creep in CLT is recent (*Park et al.*, 2006) and there are very few attempts to characterize the behaviour of rolling shear creep (*Pirvu and Karacabeyli*, 2014; *Colling*, 2014). In these works, bending tests of CLT panels are achieved and an overall creep factor is derived. It appears clearly that creep is larger with CLT than with GLT. A possible explanation may be a faster creep behaviour coming from rolling shear strains in cross layers.

This paper presents an experimental protocol to measure directly shear stiffness and creep in CLT panels. The methodology originally presented by *Perret et al.* (2018) is used to measure separately those characteristics in the rolling and the longitudinal direction. The paper is organized as follows. In Section 2, the sandwich-beam theory is recalled and the experimental set-up is introduced. In the following section, the short-term characterization of the rolling-shear stiffness modulus and the estimation of the Eurocode coefficient k_{def} (*Eurocode-5*, 2004) by means of a power law are presented. This experiment is referred as Experiment 1 and was conducted during eight months (13/03/2020 - 28/10/2020). Finally, the results of Experiment 2 (11/12/2020- 11/06/2021) are presented in Section 5 and the longitudinal shear stiffness modulus for short and long time are determined.

2 Sandwich beam theory

The rolling shear modulus $G_{r,mean}$ and the longitudinal shear $G_{l,mean}$ are characterized by means of a four-point bending test on sandwich beams constituted of a wooden core glued between two steel skins (Figure 1). The beam is simply supported on a span $d = 602$ mm and two loads $P/2$ are applied at a distance $d_0/2$ from the mid-span, with $d_0 = 200$ mm. The beam is under pure bending between these loads leading to a constant curvature. It is assumed that steel does not creep in time. The full methodology is detailed in *Perret et al.* (2018).

The sandwich beam model (*Lebée and Sab*, 2012) requires a contrast between the stiffness and the thickness of the core and skins, respectively (E_a, e_a) and (E_b, e_b) so that : $e_b \gg e_a$ and $E_a e_a \gg E_b e_b$. Because of this contrast, the bending stiffness D and the shear force stiffness F are (*Allen*, 1969):

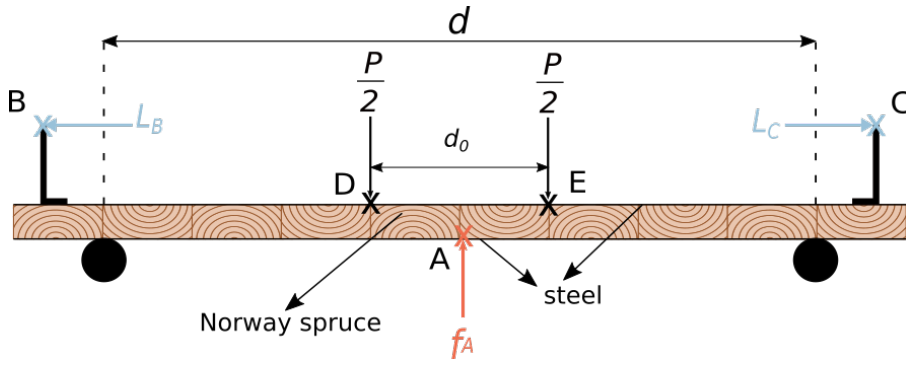


Figure 1. Four-point bending configuration on a sandwich beam, for the rolling shear configuration (experiment 1)

$$D = b \left[\frac{h^3 - e_b^3}{12} E_a + E_b \frac{e_b^3}{12} \right] \quad (1) \quad \text{and} \quad F = \frac{b(e_b + e_a)^2}{e_b} G_{r,mean} \quad (2)$$

In this paper, two shear directions are investigated. The rolling shear, or perpendicular to the grain is tested in Experiment 1. In this experiment the wooden core orientation is pictured in Figure 2. The longitudinal shear, or parallel to the grain is tested in Experiment 2. The wooden core is then rotated as pictured in Figure 1.

Whereas for Experiment 1, the contribution of the wooden core to the bending stiffness may be neglected. This is not the case for Experiment 2. Indeed, when measuring the rolling shear (Experiment 1), the contrast assumption is satisfied with $E_a = 210$ GPa and $E_b = 0.43$ GPa (litterature values). Equation 1 can be written as $D = E_a I_a + E_b I_b$. The contribution of the steel is calculated with $h = (33.5 \pm 0.4)$ mm the total thickness, $e_b = (3.9 \pm 0.4)$ mm the wood thickness, and the width of the beam $b = (41.1 \pm 0.6)$ mm. This gives $E_a I_a = (5.06 \pm 0.68)$ kN m² and the contribution of the wooden core is $E_b I_b = (44 \pm 11)$ N m². From those values, the contribution of the main core to the bending stiffness can be neglected as it contributes to less than 1%. Equation 1 can be rewritten as:

$$D = \frac{b(h^3 - e_b^3)}{12} E_a \quad (3)$$

This equation can be used in Experiment 1 to calculate the bending stiffness using the litterature value of E_a and the measured dimensions of the beam. The shear force stiffness F can be expressed as a function of the mid-span deflection f_A and the bending stiffness D :

$$\frac{1}{F} = \frac{4f_A}{P(d - d_0)} - \frac{1}{8D} \left(d^2 - \frac{1}{3}(d - d_0)^2 \right) \quad (4)$$

The measurement of f_A gives the evolution of the rolling shear modulus $G_{r,mean}$ in time. In Experiment 2, the contrast stiffness is not fulfilled but Equation 2 is still valid. The contributions of the steel and the wood are calculated with $h = (31.8 \pm 0.2)$ mm, $e_b = (29.6 \pm 0.2)$ mm, and $b = (40.6 \pm 0.2)$ mm. This gives $E_a I_a = (4.48 \pm 0.49)$ kN m² and with $E_b = 10$ GPa ; $E_b I_b = (0.88 \pm 0.21)$ kN m². The contribution of the wooden core to the bending stiffness is about 16% which can not be neglected. The bending stiffness must be precisely measured, it can be estimated from the absolute rotations at B and C (respectively φ_B and φ_C) as follows:

$$D = \frac{P(d^2 - d_0^2)}{8\Delta\varphi} \quad (5)$$

where $\Delta\varphi = \varphi_B + \varphi_C$. Equations 2 and 4 can still be used to measure the evolution of the longitudinal shear modulus $G_{l,mean}$ in time. For Experiment 2, an accurate measurement of D is necessary in order to calculate the longitudinal shear modulus and to correctly estimate its creep.

3 Methods

3.1 Specimen fabrication

Norway Spruce (*Picea abies*) boards were used to make the specimens. The layer thickness of CLT-boards in Europe are 20 mm, 30 mm and 40 mm according to *Brandner* (2013). It was chosen to use a 30 mm thick layer.

In Experiment 1, eighteen boards were glued together on their narrow edges with a wood glue (Titebond Ultimate 141/5). Glued narrow edges are not a common practice in the industry but sometimes it is used to reduce the width of the gaps. It will allow here to reduce the stress concentration in the specimens. This wooden plate was then planarized to a thickness of $e_b = 30$ mm. Then, 800 mm long specimens with a width $b = 40$ mm and a thickness $e_b = 30$ mm were cut in this plate. They were cut so that wood fibres are oriented in the transverse direction. They were conditioned at a moisture content of $u = (10.6 \pm 0.3)$ % and visually graded C24. Their density was measured to be $\rho = (495 \pm 32)$ kg m⁻³. The boards were oriented so that the pith is alternatively at the bottom or at the top which average their effect on the global behaviour (see Figure 2).

For Experiment 2 the boards used were conditioned at a moisture content of $u = (10.2 \pm 2.5)$ % and their density was measured to be $\rho = (393 \pm 53)$ kg m⁻³. Norway Spruce board of 30 × 60 mm were planarized to be 30 × 40 mm and cut to be 800 mm long oriented in the longitudinal direction.

Carbon steel XC75 sheets of Young modulus $E_a = 210$ GPa were used. They are 800 mm

long, $b = 40$ mm wide and $e_g = 1.1$ mm thick. They were sanded and glued on the top and bottom faces of the wood with a two components glue including a thixotropic epoxy based impregnating resin and adhesive (Sikadur® 300). The thickness of the glue layer is about 0.5 mm.

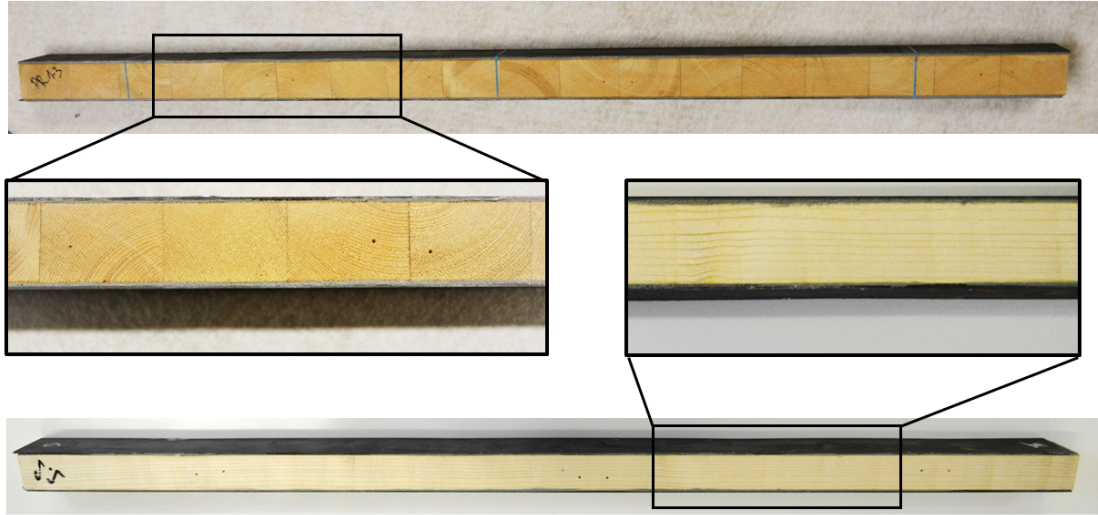


Figure 2. View of the specimens (above : Experiment 1, below : Experiment 2)

For Experiment 1, five specimens (A-E) were fabricated and six specimen (M-R) for Experiment 2. One example of each can be seen in Figure 2.

3.2 Experimental set-up

Figure 3 shows the schematic representation of the frame (0). The specimens (1) are supported on two cylinders (2) of radius $R = 23$ mm with a span $d = 602$ mm. They are loaded vertically and symmetrically by two loading fixtures (3) spaced of a length $d_0 = 200$ mm. The contact between the loading fixtures and the beam is made with a steel ball of diameter $d_b = 1.2$ mm (10). The rotation of the motor (6) drags a metal thread (9) that ascends and descends the loads (5) and the lever arms (4).

Several sensors are positioned to measure the different variables:

- Three Orbit® linear variable differential transformers (DP20S) are placed on each span of the frame (8). Two of them measure the horizontal displacement of the steel flat angles. They are represented Figure 3 as arrows L_B and L_C . The last linear variable differential transformer (LVDT) measures the vertical deflection of the beam at mid-span (f_A : arrow L_A). They have an expanded measurement uncertainty $U = 16 \times 10^{-3}$ mm.
- Two AEP transducers® S-type load cell (TS) (7) are placed in the loading fixture (3). They measure the load on points D and E . Their expanded measurement uncertainty is $U = 4.8$ N.

- Two Sensel Measurement® single axis inclinometers (SM-NA) are placed on both sides of the specimen (11). They measure the rotations φ_B and φ_C and have an expanded measurement uncertainty $U = 5 \times 10^{-3}$ rad.

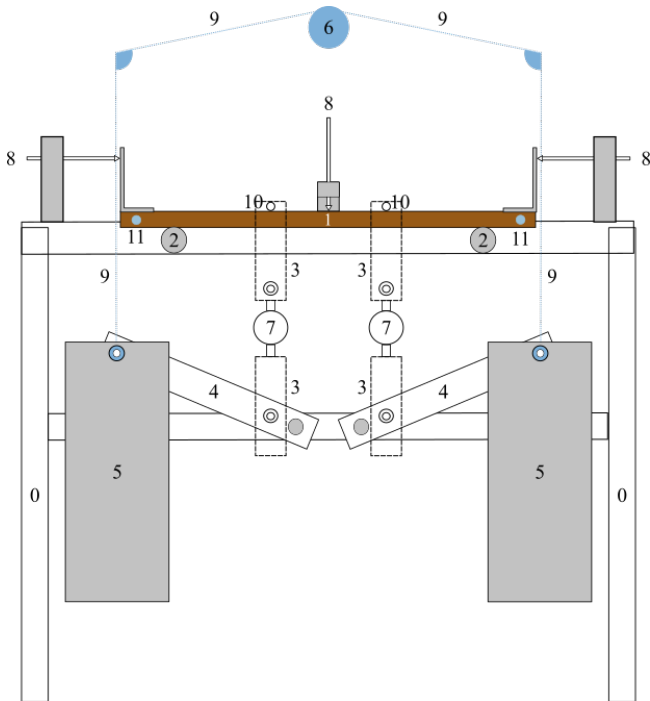


Figure 3. Framework design for the tests

In Experiment 2 the measure of the bending stiffness D is crucial to determine the instantaneous and the long term modulus. Since the inclinometers are not specifically designed for long term experiment, the LVDT sensors will be used to measure the long term displacement.

3.3 Test method

The viscoelastic limit has been well studied in the longitudinal direction (*Hoyle et al.*, 1985; *Nakai and Grossman*, 1983; *Foudjet and Bremond*, 1989; *Hayashi et al.*, 1993; *Bhatnager*, 1964; *King*, 1961) and observed to be between 40% to 50%. It is a priori not the same for the rolling-shear stiffness.

Therefore, Specimens A-E were tested under different load conditions ranging from 27 to 52 % of the characteristic shear strength $f_{r,mean} = 1.88$ MPa (*Ehrhart and Brandner*, 2018). These stress levels are approximate since the shear strength varies from one board to another. The specimens M-R loaded between 11 and 14% of the characteristic shear strength $f_{l,mean} = 7.8$ MPa (*Wood-Handbook*, 2010).

Under the viscoelastic limit, *D. G. Hunt* (1999) proposed to separate creep into three different components: pure viscoelastic (time dependent creep), mechano-sorptive creep and pseudo-creep followed by a recovery phenomenon. These components are independent but coupling effects may appear. The present experiment will be achieved such that the pure viscoelastic behaviour is isolated. Therefore, the tests were performed in

a climate-controlled room with constant temperature of $(19 \pm 1)^\circ\text{C}$ and a relative humidity in the air of $(58 \pm 8)\%$ in the first experiment. In the second experiment the temperature was $(20 \pm 1)^\circ\text{C}$ and the relative humidity in the air of $(54 \pm 6)\%$. Both times the specimens were conditioned at least one week in this room before the tests.

4 Rolling shear results

4.1 Short term

Results are plotted for beam C but are similar for all the specimens. In Figure 4 the load P is plotted as a function of the deflection f_A for the first two minutes of the experiment. A linear regression on the linear part of this curve gives an estimation of the modulus $G_{r,mean}^0$ using Equations 2 and 4 and the value of the bending stiffness calculated section 2. Table 1 summarizes the identified moduli.

Table 1. Instantaneous values

Name	$G_{r,mean}^0$ (MPa)
A	98.4
B	120
C	99.9
D	115
E	110
Moyenne	109
CoV*(%)	8.6

* Coefficient of Variation

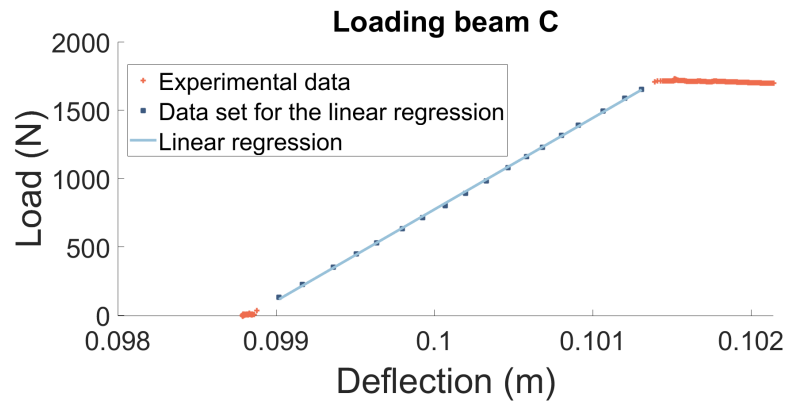


Figure 4. Applied force as a function of the mid-span deflection f_A

The cross-layer shear modulus $G_{r,mean}^0 = 109$ MPa with a coefficient of variation of 8.6% is consistent with the literature values given in Table 2. A rather high value is consistent with the sawing pattern presented in Figure 2. The coefficient of variation found is very low compared to the literature and comparable to the one already found by *Perret et al.* (2018). Indeed, the four-points bending test averages the rolling-shear stiffness on several boards.

Table 2. Short term rolling shear modulus from other experiments

Reference	MC ¹ (%)	$G_{r,mean}^0$ (MPa)	CoV ² (%)
<i>Aicher and Dill-Langer</i> (2000)	12	50	20
<i>Keunecke et al.</i> (2007)	12	53	
<i>Franzoni, Lebée, Lyon, et al.</i> (2017)		110	27
<i>Perret et al.</i> (2018)	10-13	124	6.7

¹ Moisture Content

² Coefficient of Variation

4.2 Long term

The mid-span deflections can be separated in two contributions; the bending and the shear deflection. The total mid-span deflection varies from (1.2848 ± 0.0033) mm dur-

ing the experiment. The symmetric part of the rotations varies from $(1.3 \pm 1.7) \times 10^{-3}$ rad. This variation falls within the accuracy of the LVDT. Hence, we can neglect the variations of the rotations in this experiment and calculate D .

The measured relative creep of the specimens during this experiment are plotted Figure 5 for the rolling-shear modulus $G_{r,mean}^{\infty}$. It can be observed that those curves are close to linear in a log-log scale at long time, therefore the creep can be modelled with a power law:

$$\frac{J(t)}{J_0} - 1 = mt^n \quad (6)$$

where n , m and J_0 are experimental parameters and t the time in seconds. They are independent from the load as long as it is in the linear viscoelastic domain. Indeed, wood creep has been modelled with empirical and mechanical models. Mechanical models come from the thermodynamics (Schapery, 1966). They are systems composed of Kelvin and Maxwell elements. Those models are useful to differentiate the several creep components: elastic, viscous and viscoelastic. They are mostly used to model creep occurring with climate changes (Varnier, 2019; Mukudai, 1983; D. Hunt and Gril, 1994). Empirical models are power or logarithmic functions and they fit and predict well those phenomena. Youngs (1957) was the first to model wood creep from a 3-days experiment as a power law similar to the Equation 6. Clouser (1959) and Gressel (1984) used this same equation to fit their 10-year creep tests. It has been widely used since then to fit and predict creep wood behaviour (Sugiyama, 1957; Schniewind, 1966; Hayashi et al., 1993).

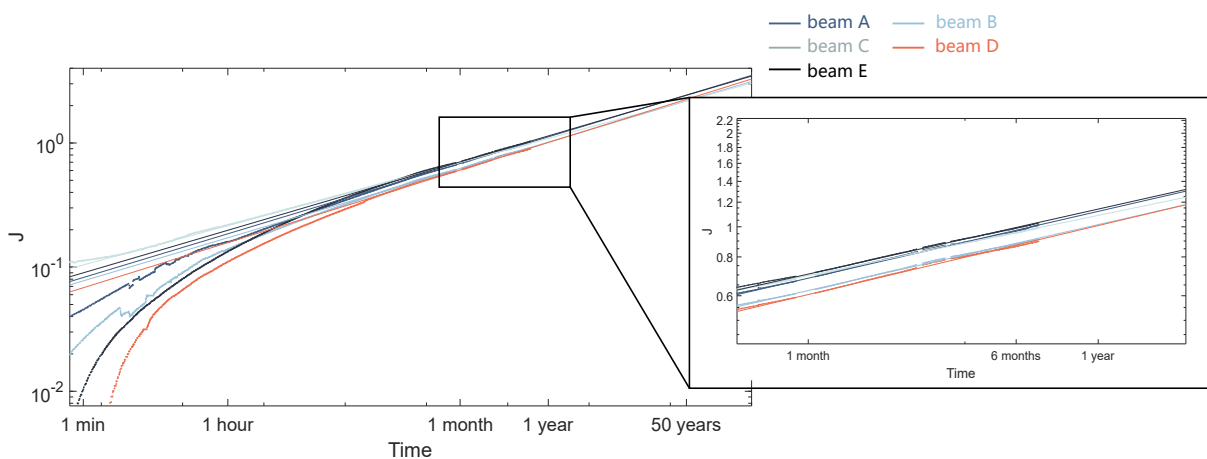


Figure 5. Rolling-shear relative creep curves and power law fittings

In international standards the design of buildings has to be estimated for 50-years. Therefore, a prediction model is required to extrapolate a value of the deflection of wood at such time period. In the Eurocode, this is taken into account by means of the coefficient k_{def} which corresponds to the relative creep at 50-years. Considering exclu-

sively rolling shear deformations, we define k_{def}^{GR} as:

$$G_{r,mean}^{\infty} = \frac{G_{r,mean}^0}{1 + k_{def}^{GR}} \quad (7)$$

with $G_{r,mean}^0$ the short-term rolling shear modulus and $G_{r,mean}^{\infty}$ the secant rolling-shear modulus in 50 years. A linear regression was done on the logarithmic values. The k_{def}^{GR} values found are summarized in Table 3 with a mean value of 2.43 and a coefficient of variation equal to 6.18 % which corresponds approximately to the coefficient of variation of the instantaneous modulus. The stress level does not seem to have a significant influence on k_{def}^{GR} which comforts the assumption of linear visco-elasticity.

Table 3. Values of k_{def}^{GR}

Name	k_{def}^{GR}
A	2.59
B	2.44
C	2.22
D	2.34
E	2.54
Mean	2.43
CoV*(%)	6.18

* Coefficient of Variation

Table 4. Fitting coefficients values

Name	J_0	n	m
A	92.8	0.210	0.0302
B	113	0.212	0.0274
C	88.9	0.217	0.0224
D	107	0.211	0.0266
E	106	0.194	0.0422

The values found for the coefficient of Equation 6 are shown in Table 4. They fall into the range of coefficients found in the literature and summarized in (Tong et al., 2020).

5 Longitudinal results

5.1 Short term

The value of the instantaneous bending stiffness is measured with the inclinometers during the loading of each specimen. The load is plotted against the symmetric part of the rotations during the loading Figure 6. Results are plotted for beam N and are similar for all specimens. A linear regression on the linear part of this curve allows to determine the bending stiffness D . The results are summerized Table 5. They are in the scope of the calculus that was presented in Section 2.

Using Equations 2 and 4 the value of the instantaneous longitudinal shear modulus can be calculated. It is deduced from the slope of the function between the load P and the mid-span deflection f_A . The values found are summerized in Table 5 and, except for beam O , the results are consistent. The coefficient of variation found for the longitudi-

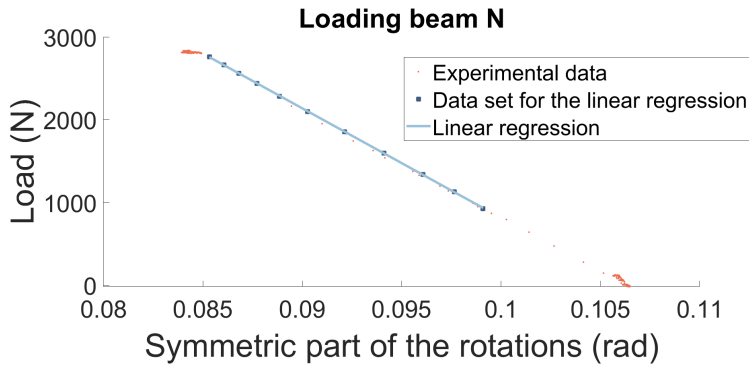


Figure 6. Load P function of the symmetric part of the rotation $\Delta\varphi$, beam N

nal shear is in the scope of the variation of the wood which is about 20%.

Table 5. Instantaneous values for longitudinal shear

Name	M	N	O	P	Q	R	Mean	CoV*(%)
D^0 (kN m ²)	5.71	5.26	5.81	5.13	5.21	4.98	5.35	6.2
$G_{l,mean}^0$ (MPa)	425	385	229	359	384	355	356	19

* Coefficient of Variation

5.2 Long term

The long term part of the long term mid-span deflection is (0.2959 ± 0.0033) mm while it was (1.2848 ± 0.0033) mm for the rolling-shear. It is much smaller than in the previous experiment and therefore require a more precise analysis. The bending and shear contribution to the mid-span bending can be separated as:

$$f_A = \frac{k_1}{F} + \frac{k_2}{D} \quad (8)$$

where k_1 and k_2 are two coefficients that can be determined with Equation 4 and are constant during the whole experiment.

The long term symmetric part of the rotations is $(1.4 \pm 1.7) \times 10^{-3}$ rad. This variation falls into the uncertainty of the sensors and could be neglected. If this variation is not neglected the bending contribution on the mid-span creep deflection is then about 45%. This contribution may be associated to the creep of the wood Young modulus E_b in the longitudinal direction with Equation 1.

Hence, two estimations of k_{def}^{GL} are proposed here ; one considering that only the shear contributes to the creep of the long term mid-span deflection f_A and one considering that there is a bending creep as well. In the first case, D is assumed constant in Equation 8, while in the second case, D is taken from the long term measurement. In both cases, considering the deformations in the longitudinal direction, we define a creep coefficient k_{def}^{GL} as :

$$G_{l,mean}^{\infty} = \frac{G_{l,mean}^0}{1 + k_{def}^{GL}} \quad (9)$$

with $G_{l,mean}^0$ the short-term longitudinal shear modulus, $G_{l,mean}^{\infty}$ the longitudinal shear modulus in 50 years.

Using the power law Equation 6, a linear regression was fitted on the logarithmic values. Figure 7 shows the fitting of the data when assuming that there is no bending creep (D is constant). The cycles visible corresponds to those of the air conditioning that regulated the temperature of the room during the experiment. Those variations correspond to the sensitivity of the LVDT sensors to temperature. They exist in Experiment 1 but are not visible in Figure 5 as the creep deflection is 4 times larger. The values of k_{def}^{GL} are summarized Table 6 with a mean value of 1.1 (CoV = 15%).

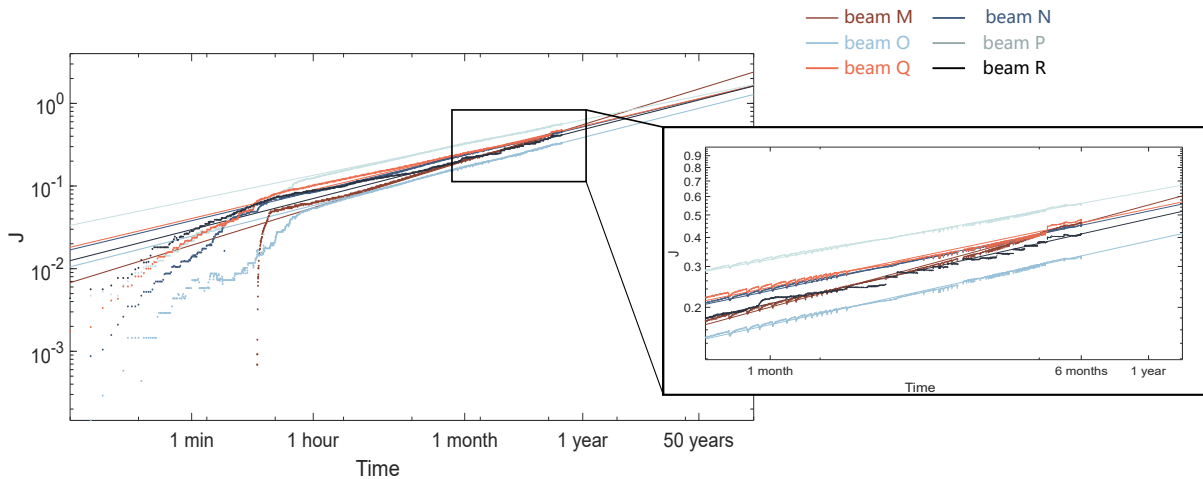


Figure 7. Fitted data, longitudinal creep of $G_{l,mean}$ considering that there is only a shear creep

A similar fitting was done when considering that the bending contributes to the creep of the mid-span. There was a power outage the second month of the experiment and the measure of the rotation of the beam M was lost. Therefore no creep results are presented for this specimen in this case. The results are in Table 6 and k_{def}^{GL} is calculated with a mean value of 0.6 (CoV = 26%).

Table 6. Values of k_{def}^{GL}

Name	M	N	O	P	Q	R	Mean	CoV*(%)
k_{def}^{GL}	–	0.84	0.52	0.68	0.46	0.51	0.60	26
k_{def}^{GL} (without bending creep)	1.4	1.1	0.88	1.2	1.1	1.1	1.1	15

* Coefficient of Variation

In both estimations, the stress level seems not to have any influence on the creep which validates the hypothesis of linear visco-elasticity. Experiments are still going on to better understand those results and obtain a more precise value of k_{def}^{GL} .

6 Conclusions

The value found in the current version of the Eurocode of the creep coefficient k_{def} is 0.6. This value is the same for all orthotropic elastic moduli (*Eurocode-5*, 2004). The value of the rolling shear coefficient k_{def}^{GR} identified in the present experiment is 2.43 while the value of the longitudinal shear coefficient k_{def}^{GL} is between 0.60 and 1.1. This gives an approximated range of k_{def}^{GL} but seems to indicate that this creep is comparable to the creep of the bending stiffness in the longitudinal direction E_b . The rather large value of the rolling-shear coefficient is not inconsistent and was expected considering previous attempts to estimate k_{def} for CLT panels (*Pirvu and Karacabeyli*, 2014; *Colling*, 2014). Indeed, the deflection of a CLT panel is the superposition of the bending and the shear deflection. The shear contribution in the global creep depends on the slenderness of the panel and varies from 30% of the total deflection for thick panels to few percent for slender panels. Hence, a distinction between the different deformation types might be necessary to have a better estimation of the long term deflection in CLT panels. Indeed, the present results clearly indicate that rolling shear creeps faster than longitudinal shear. More experimental campaigns need to be performed to obtain statistically significant results. If the present value is confirmed it could have consequences for the design of CLT and other timber products. For instance, this may lead to more accurate design guidelines either for serviceability limit state (SLS) or long-term buckling strength of CLT walls, which completes recent recommendations for more accurate modelling (*Franzoni, Lebée, Lyon, et al.*, 2017; *Franzoni, Lebée, Forêt, et al.*, 2015; *Perret et al.*, 2018).

7 References

- Aicher, S. and G. Dill-Langer (2000). "Basic considerations to rolling shear modulus in wooden boards." en. In: 11, p. 10.
- Allen, H. (Oct. 1969). *Analysis and Design of Structural Sandwich Panels: The Commonwealth and International Library: Structures and Solid Body Mechanics Division*. en. Elsevier.
- Bhatnager (1964). "Creep in wood in tension parallel to grain." In: *Holz als Roh- und Werkstoff*.
- Brandner, R. (2013). "Production and Technology of Cross Laminated Timber (CLT): A state-of-the-art Report." en. In: p. 33.
- Brandner, R., G. Flatscher, A. Ringhofer, G. Schickhofer, and A. Thiel (May 2016). "Cross laminated timber (CLT): overview and development." en. In: *European Journal of Wood and Wood Products* 74.3, pp. 331–351.
- Clouser, W. S. (1959). "Creep of small wood beams under constant bending load." en. In.

- Colling, F. (2014). "Creep behavior of cross laminated timber in service class 2." en. In: *Technical Report*. Hochschule Augsburg, University of Applied Science, p. 10.
- Ehrhart, T. and R. Brandner (2018). "Rolling shear: Test configurations and properties of some European soft- and hardwood species." en. In: *Engineering Structures* 172, pp. 554–572. DOI: 10.1016/j.engstruct.2018.05.118.
- Eurocode-5 (2004). *Design of timber structures*.
- Foudjet, A. and C. Bremond (1989). "Creep of four tropical hardwoods from Cameroon." en. In: *Wood Science and Technology* 23.4, pp. 335–341. DOI: 10.1007/BF00353249.
- Franzoni, L., A. Lebé, G. Forêt, and F. Lyon (Aug. 2015). "Advanced modelling for design helping of heterogeneous CLT panels in bending." In: *International Network on Timber Engineering Research*. Sibenik, Croatia.
- Franzoni, L., A. Lebé, F. Lyon, and G. Forêt (Sept. 2016). "Influence of orientation and number of layers on the elastic response and failure modes on CLT floors: modeling and parameter studies." en. In: *European Journal of Wood and Wood Products* 74.5, pp. 671–684. DOI: 10.1007/s00107-016-1038-x.
- (June 2017). "Elastic behavior of Cross Laminated Timber and timber panels with regular gaps: Thick-plate modeling and experimental validation." en. In: *Engineering Structures* 141, pp. 402–416. DOI: 10.1016/j.engstruct.2017.03.010.
- Gressel, P (1984). "Zur Vorhersage des langfristigen Form inderungsverhaltens aus Kurz-Kriechversuchen." de. In: p. 9.
- Hayashi, K., B. Felix, and C. Le Govic (1993). "Wood viscoelastic compliance determination with special attention to measurement problems." en. In: *Materials and Structures* 26.6, pp. 370–376. DOI: 10.1007/BF02472963.
- Hoyle, R., M. Grzfith, and R. Itani (1985). "Primary Creep in Douglas-fir beams of commercial size and quality." en. In: *Wood and Fiber Science* 17.3, pp. 300–314.
- Hunt, D and Joseph Gril (1994). "Possible contribution of fibre slippage to the longitudinal creep of wood." In.
- Hunt, D. G. (1999). "A unified approach to creep of wood." en. In: *Proceedings of the Royal Society of London. Series A: Mathematical, Physical and Engineering Sciences* 455.1991, pp. 4077–4095. DOI: 10.1098/rspa.1999.0491.
- Keunecke, D., W. Sonderegger, K. Pereteanu, T. Lüthi, and P. Niemz (Apr. 2007). "Determination of Young's and shear moduli of common yew and Norway spruce by means of ultrasonic waves." en. In: *Wood Science and Technology* 41.4, pp. 309–327.
- King, E G (1961). "Time-Dependent Strain Behavior of Wood." en. In: *Forest Products Journal*, p. 5.
- Krabbe, E (1960). "Messungen von Gleit- und Dehnungszahlen an Holzstäbchen mit rechteckigen Querschnitten." allemand. PhD thesis. Hannover.
- Lebé, A. and K. Sab (Apr. 2012). "Homogenization of cellular sandwich panels." en. In: *Comptes Rendus Mécanique* 340.4-5, pp. 320–337.
- Mukudai, J. (1983). "Evaluation on non-linear viscoelastic bending deflection of wood." en. In: *Wood Science and Technology* 17.1, pp. 39–54. DOI: 10.1007/BF00351831.

- Nakai, T and P. U. A. Grossman (1983). "Deflection of wood under intermittent loading." en. In: *Wood Science and Technology* 17, pp. 55–67.
- Park, H., M. Fushitani, K. Sato, T. Kubo, and H. Byeon (June 2006). "Bending creep performances of three-ply cross-laminated woods made with five species." en. In: *Journal of Wood Science* 52.3, pp. 220–229. doi: 10.1007/s10086-005-0750-7.
- Perret, O., A. Lebéé, C. Douthe, and K. Sab (Oct. 2018). "Experimental determination of the equivalent-layer shear stiffness of CLT through four-point bending of sandwich beams." en. In: *Construction and Building Materials* 186, pp. 1132–1143.
- (May 2019). "Equivalent stiffness of timber used in CLT: closed-form estimates and numerical validation." en. In: *European Journal of Wood and Wood Products* 77.3, pp. 367–379. doi: 10.1007/s00107-019-01395-x.
- Pirvu, Ciprian and Erol Karacabeyli (2014). "Time-dependent behaviour of CLT." en. In: p. 2.
- Schapery, R.A. (1966). "An engineering theory of nonlinear viscoelasticity with applications." en. In: *International Journal of Solids and Structures* 2.3, pp. 407–425.
- Schniewind, Arno P. (1966). "On the influence of moisture content changes on the creep of beech wood perpendicular to the grain including the effects of temperature and temperature changes." de. In: *Holz als Roh- und Werkstoff* 24.3, pp. 87–98.
- Sugiyama, H. (1957). "The creep deflection of wood subjected to bending under constant loading." en. In: *Transactions of the Architectural Institute of Japan* 55.0, pp. 60–70.
- Tong, D., S. Brown, D. Corr, and G. Cusatis (2020). "Wood creep data collection and unbiased parameter identification of compliance functions." en. In: *Holzforschung* 0.0.
- Varnier, Maximin (2019). "Comportement thermo-hygro-mécanique différencié des feuillus." fr. PhD thesis.
- Wood-Handbook (2010). *Wood Handbook, Wood as an Engineering Material*. en. U.S. Dept. of Agriculture, Forest Service, Forest Products Laboratory.
- Youngs, Robert L (1957). "The Perpendicular-to-grain mechanical properties of red oak as related to temperature, moisture content and time." en. PhD thesis.
- Zhou, Q., M. Gong, Y. Chui, and M. Mohammad (Aug. 2014). "Measurement of rolling shear modulus and strength of cross laminated timber fabricated with black spruce." en. In: *Construction and Building Materials* 64, pp. 379–386.